

Aggregate Ramp Rates Analysis of Distributed PV Systems in San Diego Gas & Electric Territory

Mohammad Jamaly, Juan L Bosch, and Jan Kleissl

Dept. of Mechanical and Aerospace Eng., University of California, San Diego

March 15, 2013

Abstract

Aggregate ramp rates of 45 distributed photovoltaic (PV) systems installed in San Diego, CA and surrounding area were analyzed and compared to modeled power calculated from irradiance estimated from satellite. Irradiance measured at 5 ground stations is considered as well. The goal was to quantify the largest aggregate ramp rates and evaluate how much on-line metering and telemetry of PV systems is necessary to track output of distributed generation for resource-adequacy applications. Over one year the largest hourly aggregate absolute ramp was a 60% increase and hourly ramps over 28% occurred only about once per day (all ramps are expressed as a fraction of Performance Test Conditions (PTC) rating). The effects of specific meteorological conditions, such as coastal marine layer clouds and frontal system effects, on occurrence of large ramps were investigated over the area using satellite imagery. Evaporation of morning marine layer clouds caused a disproportionately large amount of up-ramps.

1. Introduction

Integration of large amounts of photovoltaic (PV) into the electricity grid poses technical challenges due to the variable solar resource. Solar distributed generation (DG) is often behind the meter and consequently invisible to grid operators. The ability to understand actual variability of solar DG will allow grid operators to better accommodate the variable electricity generation for resource adequacy considerations that inform scheduling and dispatching of power. From a system operator standpoint, it is especially important to understand when

aggregate power output is subject to large ramp rates. If in a future with high PV penetration all PV power systems were to strongly increase or decrease power production simultaneously, it may lead to additional cost or challenges for the system operator to ensure that sufficient flexibility and reserves are available for reliable operations.

In this study, aggregate ramp rates of distributed PV systems installed in San Diego, CA and surrounding area is analyzed. Measured and modeled irradiation data along with power output of PV systems are applied to evaluate the frequency, magnitude, and ability to track large ramps in the aggregate power output. The methodology is described in Section 2. Results of the detected largest ramps in aggregate power output are presented in Section 3 and Section 4 contains the conclusions.

2. Methodology

2.1. Datasets

The California Solar Initiative (CSI) rebate program requires a performance-based-incentive (PBI) payout for systems larger than 30 kW and makes it optional for smaller systems [1]. This requires metering and monthly submission of 15 minute energy output to the payout administrator. We have obtained the 2010 CSI measured output (P_{CSI}) - quality controlled for system performance [2] - for 194 PV power plants in San Diego Gas & Electric (SDG&E) territory (referred to as investor-owned utility, IOU).

The CSI database also includes street address and PV system specifications including DC Rating (kW_{DC}) at standard test condition (STC), AC Rating (kW_{AC}) at performance test condition (PTC, typically 14% less than STC), module and inverter models, inverter maximum efficiency, panel azimuth and tilt angles, and tracking type. The STC rating is obtained under idealized, controlled conditions of 1000 W m^{-2} plane-of-array irradiance and cell temperature at 25°C while the PTC simulates more realistic conditions at 1000 W m^{-2} plane-of-array irradiance with panel temperature derived from ambient air temperature at 20°C and 1 m s^{-1} wind speed. Given the rapid increase in solar distributed generation (DG) in most coastal urban centers in California (like San Diego which is included in this study), this dataset is complete enough to project future effects of high PV penetration on the electric grid.

Quality control [3] was used to exclude all CSI sites with at least one of the following characteristics not representative of irradiance: PV systems with hourly averaged (versus 15 min)

data, more than 70% missing data (mostly because they were installed during 2010), significant noise or large spikes in power due to recording issues, decrease in power due to soiling, significant clipping of power due to undersized inverters, less than 5 distinct power output for the whole year, or plants divided into sub-arrays with different panel tilt and azimuth angles. Therefore, a final set of 45 PV systems with total PTC rated capacity of 4.75 MW, mean PTC rated of 101 kW, and median PTC rated of 38.7 kW are analyzed (Fig. 1).

For comparison, ground measured irradiation data from the California Irrigation Management Information System (CIMIS) with 124 active weather stations are considered [4]. GHI is reported as an hourly average of 60 measurements within the hour [4]. Each CIMIS station is equipped with a Li-Cor LI200S photodiode pyranometer, accurate under typical conditions to $\pm 5\%$ (CIMIS, 2009b). CIMIS provides an initial QC assessment based on procedures described in [5], issuing flags that allow the user to remove any data that appears erroneous. These flags, detailed on the CIMIS website [4], restrict any data that contain obvious outliers or unphysical characteristics. CIMIS provides a further description of the QC method in the CIMIS technical manual [6]. The best 5 CIMIS stations (Fig. 1) are considered in this study according to further quality control in [7]. Unfortunately, however, the CIMIS data could not be applied in an operational environment, because station data are only downloaded once per day at midnight. Nevertheless, the data can elucidate whether ground measurement networks (such as those installed in SMUD and SDG&E territories) are beneficial in tracking PV output.

Modeled GHI is provided by Clean Power Research's commercially available SolarAnywhere (SAW) derived from Geostationary Operational Environmental Satellite (GOES) visible imagery [8]. To obtain GHI, a cloud index is calculated for each pixel from the reflectance measured by the satellite. Instantaneous, spatially averaged GHI is then calculated by using the cloud index along with a clear sky model that considers local and seasonal effects of turbidity [9]. SAW enhanced resolution satellite-derived irradiation with 30-min temporal and 1 km spatial resolutions is applied in this study. SAW can be purchased for operational applications with less than 30 min latency.

At each PV system, the CSI measured power output (P_{CSI}) is compared with the measured GHI at the closest CIMIS (GHI_{CIMIS}) station as well as the SAW estimated GHI (GHI_{SAW}) and power output (P_{SAW}) of the pixel in which the PV system is located. P_{SAW} is obtained by converting irradiation data into power output using a performance model as described in [10].

The analysis is conducted for January 1st to December 31st, 2010. To avoid errors due to sensor cosine response and shading by nearby obstructions (not considered by SAW), only data for solar zenith angles less than 75° are considered. Performance when the solar zenith angle is less than 75° for a flat plate system is less than 26% of rated capacity so hourly change rates are likely to be substantially less during those periods’.

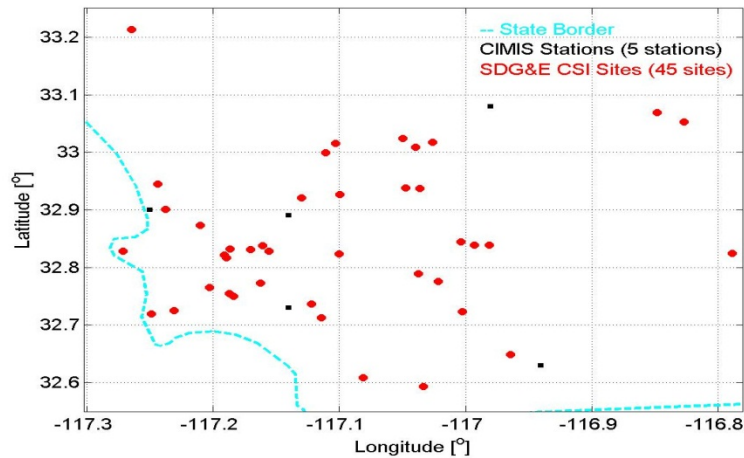


Fig. 1: Map of Sites: Map of 45 PV systems in SDG&E territory along with 5 CIMIS stations within that area under investigation.

2.2. Aggregate PV Ramp Rates

The objective of the ramp rate analysis is two-fold. Firstly, knowledge about the largest possible aggregate ramp rates and underlying meteorological conditions is useful for system operators to plan for worst-cases. Secondly, under extreme ramp rate conditions, knowing the PV output in real time would be most valuable since regulation up or regulation down capacity may have to be quickly procured. The ability of CIMIS and SAW modeled PV performance to match actual output is therefore of interest.

2.2.1. Absolute ramp rates

The aggregate CSI measured power output for the 45 PV systems is used to determine the largest absolute ramp rates in 2010. First, on each day, the aggregate PV power output is calculated at each time step; PV sites with any missing data on that day are completely excluded. Differences in the aggregate PV power output are calculated for different ramp duration intervals; 15-min through 5-hour in 15-min increments.

We present normalized absolute ramp rates to facilitate scaling the results to future PV penetration scenarios (assuming a similar geographic diversity). Therefore, the aggregate power outputs are normalized by the aggregate (PTC) kW_{AC} capacity of the PV systems for each time period (Figs. 2, 3). Also to facilitate the comparison between CIMIS and SAW irradiances, and CSI power output, each timeseries is normalized by the respective maximum daily values (normalized to a maximum of 1 for each day in Fig. 5).

To determine whether the largest absolute ramp rates are as a result of diurnal cycles, 1-min GHI in clear sky conditions (GHI_{CS}) at each PV site is calculated based on the Ineichen model with Linke Turbidity from the SoDa database [9],[11],[12]. Then, GHI_{CS} is averaged over the CSI time interval (15-min). The aggregate GHI_{CS} is calculated at each time step and differences in the aggregate GHI_{CS} are also calculated for different ramp duration intervals; 15-min through 5-hour in 15-min increments.

2.2.2. Weather-induced ramp rates

Ramp rates with reference to a 30-day average of power output, on the other hand, are helpful to detect unexpected variations. These unexpected variations are more likely caused by weather than the sun's movement through the sky. First the average aggregate PV power output of the previous 30 days at a given time of day (ToD), corrected for differences in aggregate PV capacity, is subtracted from the aggregate PV power output at that ToD. Then, the differences in the resulting timeseries constitute weather-induced ramp rates, which are calculated for different ramp duration intervals; 15-min through 5-hour in 15-min increments. Weather-induced ramp rates are either normalized by the aggregate kW_{AC} capacity of the PV systems (Figs. 3, 7) or by the respective maximum daily values (normalized to a maximum of 1 for each day in Fig. 9).

2.3. Temporal Interpolation between Datasets

SolarAnywhere provides 30-min centered irradiation at :00 and :30. CSI provides 15-min averaged power output with an interval-ending timestamp at :00, :15, :30, and :45. So, for statistical analysis, two CSI intervals are aggregated to compare against the corresponding SAW interval.

2.4. Error Metrics

Mean Bias Error (MBE) describes persistent differences between P_{SAW} and P_{CSI} . Mean Absolute Error (MAE) and Root Mean Square Error (RMSE) describe random differences between P_{SAW} and P_{CSI} . MBE, MAE, and RMSE are calculated as

$$\left\{ \begin{array}{l} MBE = \frac{1}{N} \sum_{n=1}^N (P_{SAW} - P_{CSI}) \\ MAE = \frac{1}{N} \sum_{n=1}^N abs(P_{SAW} - P_{CSI}) \\ RMSE = \frac{1}{N} \sqrt{\sum_{n=1}^N (P_{SAW} - P_{CSI})^2} \end{array} \right. \quad \text{Eq. (1),}$$

where N is the number of samples. Also, the relative MBE (rMBE), relative MAE (rMAE), and normalized RMSE (nRMSE) are calculated as

$$\left\{ \begin{array}{l} rMBE = \frac{MBE}{mean(P_{CSI})} * 100\% \\ rMAE = \frac{MAE}{mean(P_{CSI})} * 100\% \\ nRMSE = \frac{RMSE}{mean(P_{CSI})} * 100\% \end{array} \right. \quad \text{Eq. (2).}$$

For 2010, the bias error between P_{SAW} and P_{CSI} was found to be larger in summer (up to 5% rMBE) while SAW underestimates the measured data in the other months [10].

3. Results

3.1. Absolute ramps

3.1.1. Absolute ramp rates in aggregate output and clear sky irradiance by time horizon

The largest step sizes in the absolute aggregate PV power output (normalized by kW_{AC}) and the aggregate GHI_{CS} (normalized by 1000 W m^{-2}) are detected over the year for different intervals (Fig. 2). As expected, the maximum ramp magnitude increases with the ramp interval. The maximum ramp magnitude approach 90% for 5 hour ramps reflective of the diurnal cycle (e.g. from zero output at 0700 to near maximum output at 1200) on a clear day.

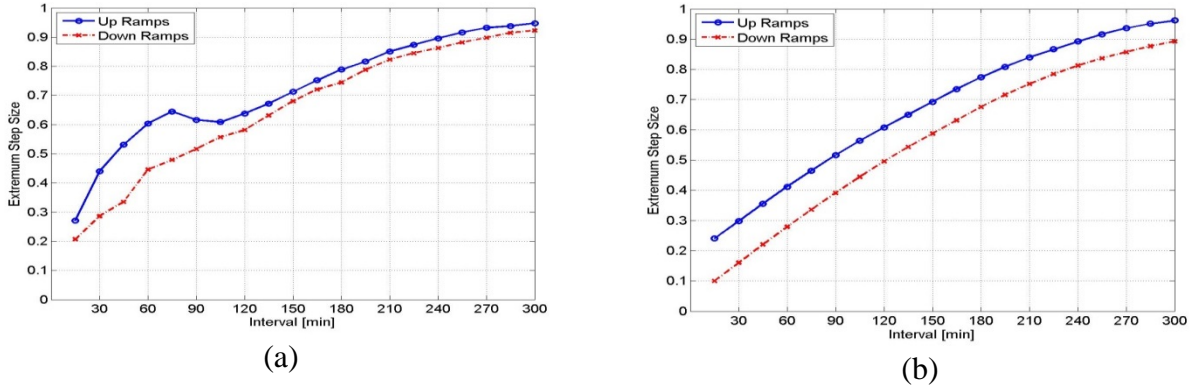


Fig. 2: Largest absolute ramps: Largest ramp magnitude versus ramp time interval (from 15-min upto 5-hours) for aggregate (a) normalized output (P_{CSI}/kW_{AC}) and (b) clear sky GHI ($GHI_{CS}/1000 \text{ W m}^{-2}$) from all 45 PV sites.

3.1.2. Histogram of large absolute hourly ramps

1-hour ramps have a special significance as most energy exchange between electric balancing areas is currently scheduled over hourly intervals. The distribution of hourly ramp rates in normalized aggregate measured PV power output along with 1-hour ramp rates in the aggregate clear sky GHI ($GHI_{CS} / 1000 \text{ W m}^{-2}$) are presented in Fig. 3. The clear sky rate is of interest because it simulates the output ramps that would be experienced if there were no clouds or fog and the weather was always clear. This is the precisely predictable rate that is not governed by weather.

The distribution of hourly absolute ramp rates in the aggregate PV output (Fig. 3) shows that ramps over $28\% \text{ h}^{-1}$ of PTC capacity are rare, occurring only for 150 hours of the year. For smaller ramps, the distribution decreases linearly.

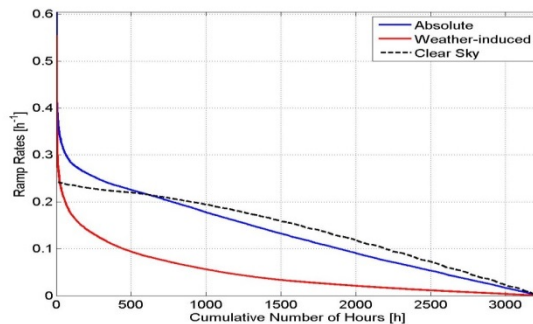


Fig. 3: Distribution of hourly ramp rates: Cumulative distribution of absolute value of 1-hour ramp rates of aggregate absolute and weather-induced 15-min output (both normalized by kW_{AC}) and clear sky GHI ($GHI_{CS}/1000 \text{ W m}^{-2}$) from all 45 PV sites. The ramps are zero for the remaining hours up to 8760 h, because these are night time conditions or missing data.

Fig. 4 shows a histogram (by month) of the 1-hour absolute ramp rates of aggregate normalized power output (normalized by kW_{AC}) which are larger than 28% of PV capacity.

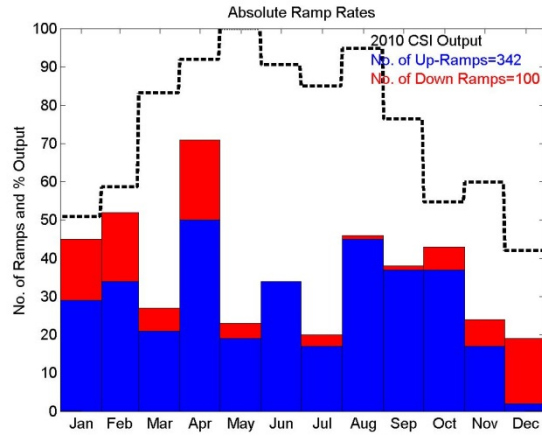


Fig. 4: Month of occurrence and direction of large absolute ramps: Histogram of the largest 1-hour ramp rates of aggregate absolute 15-min output (P_{CSI}/kW_{AC}) from all 45PV sites. The black lines show percentage of the measured aggregate 15-minute PV output from all 195 PV sites normalized to the maximum month (May).

3.1.3 Days with the largest hourly absolute ramps

Fig. 5 shows daily profiles of the normalized aggregate CSI measured and SAW modeled power outputs along with the normalized aggregate CIMIS GHI (all normalized to a maximum of 1 as described in Section 2.2) for the days when the four largest absolute ramps were observed. The largest ramp caused a change of 60% of PTC capacity within one hour. SAW estimates tracked the CSI power output typically within 1-12% rMAE at 30-min resolution. Daily profiles of the aggregate CSI measured and SAW modeled power outputs (normalized by PTC capacity) along with the aggregate SAW and CIMIS GHI (divided by 1000 W m^{-2}) for the four days in Fig. 5 are presented in Appendix A, Fig. A1. The 15 minute consecutive GOES images for the time period with the largest absolute ramp (Figs. 5a) are illustrated in Fig. 6.

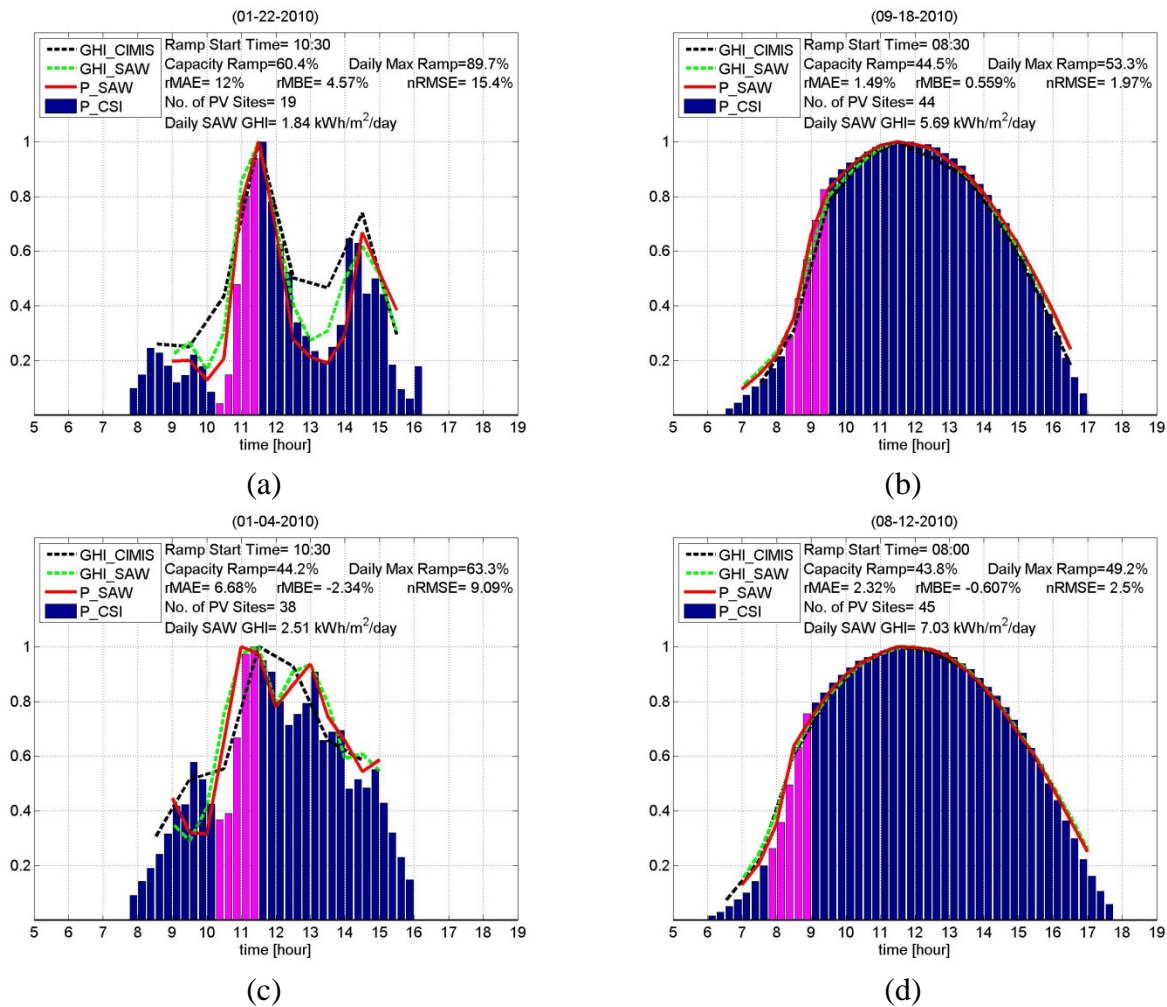


Fig. 5: Four days with largest absolute ramps: Normalized aggregate 15-minute PV output from all 45 PV sites (bars) for the days with the largest 1-hour ramp rates in 2010 (magenta bars show the timing of the large ramp). Normalized (to a maximum of 1) aggregate 30-minute performance output (red) and GHI (green) obtained from SolarAnywhere at each pixel and normalized aggregate hourly measured GHI of 5 weather stations (black) are also shown. The caption indicates the daily available GHI from SolarAnywhere averaged over all 45 PV sites, the CSI ramp magnitudes (normalized by both PV PTC capacity and daily maximum output). Relative (divided by annual average CSI output) mean absolute error (MAE), mean bias error (MBE), and RMSE between aggregate SAW performance and CSI outputs are also presented. (a) Jan. 22, 2010, (b) Sep. 18, 2010, (c) Jan. 4, 2010, (d) Aug. 12, 2010.

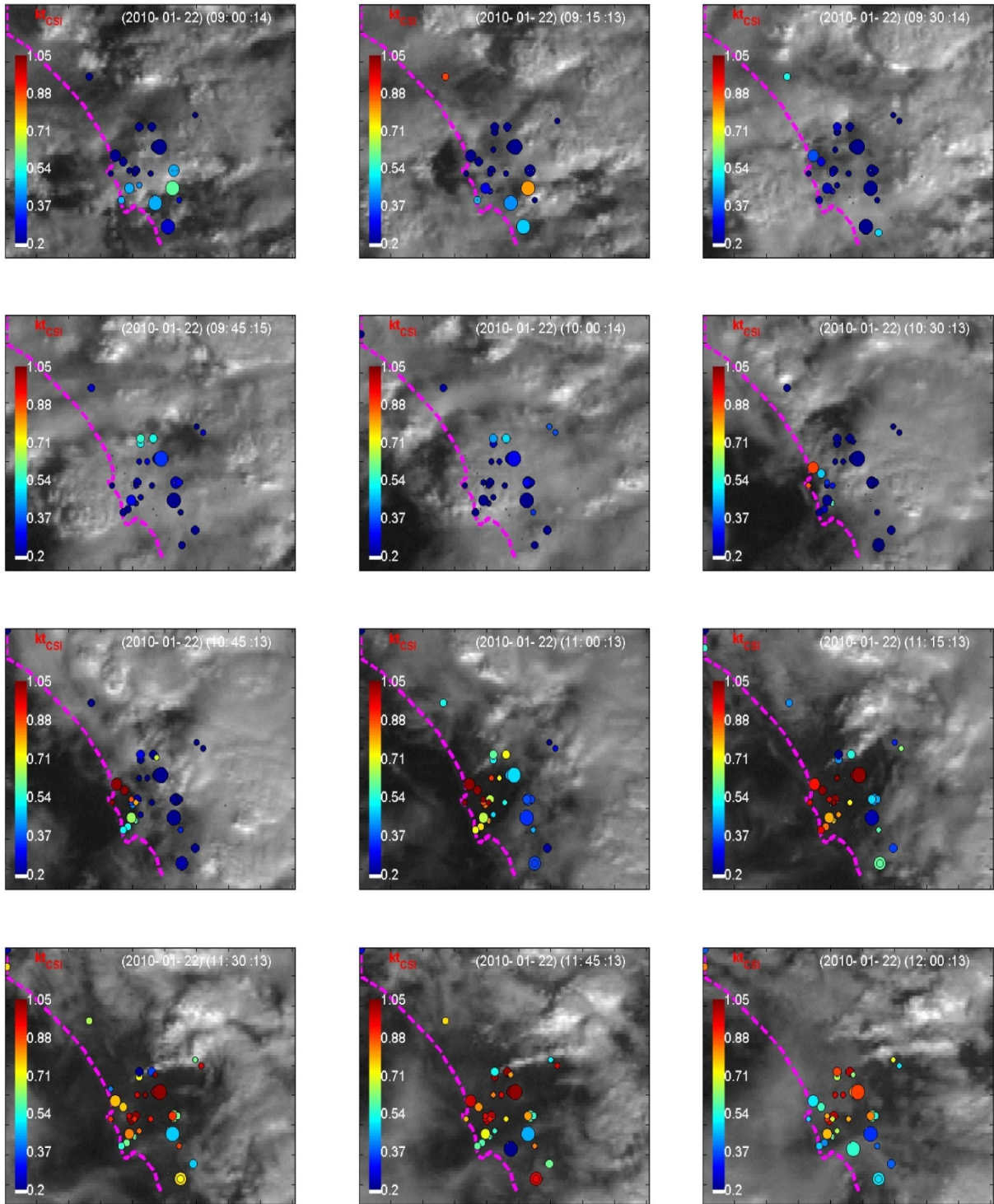


Fig. 6: GOES images for the days with the largest ramp: GOES satellite images at 15 minute resolution on Jan. 22, 2010 (Fig. 5a). The circles represent 45 PV systems shown in Fig. 1. The area of the circles is proportional to the power rating of the PV system and the largest system is 501 kW. The color bar shows the ratio of 15-min averaged output to annual maximum output at that time of day (ToD).

3.2. Weather-induced ramps

3.2.1. Weather-induced ramp rates by time horizon

Similar to Fig. 2, the largest step sizes in the weather-induced aggregate ramp rates (normalized by kW_{AC}) is presented in Fig. 7.

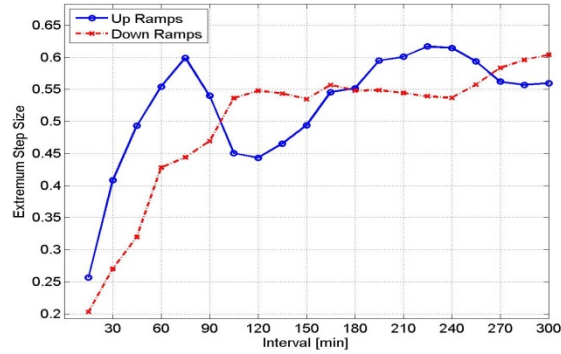


Fig. 7: Largest weather-induced ramps: same as Fig. 2 but for weather-induced normalized ramps (normalized by kW_{AC}).

3.2.2. Histogram of large weather-induced ramps

The distribution of 1-hour weather-induced ramp rates in the aggregate PV output (Fig. 3) shows that ramps over $16\% \text{ h}^{-1}$ of PTC capacity are rare.

Fig. 8 shows a histogram (by month) of the 1-hour weather-induced ramp rates of aggregate normalized power output (normalized by kW_{AC}) which is larger than 16% of PV capacity. The large weather-induced ramps were most likely in the spring and winter months (primarily December and January) when they occurred about once per day. Presumably, this is related to overcast conditions (large morning down or evening up-ramp compared to the 30 day – mostly clear - average) or when storm systems moving into (large down ramp) or out of the area (large up-ramp). Large ramps are anti-correlated with the average output over a month.

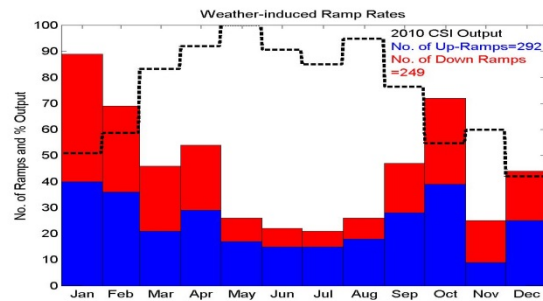


Fig. 8: Month of occurrence and direction of large weather-induced ramps: Same as Fig. 4a but for weather-induced ramps.

3.2.3. Days with the largest hourly weather-induced ramps

The days when the four largest weather-induced ramps (with reference to 30-days average of the aggregate output as described in Section 2.2) were calculated. January 22 was both the day with the largest weather-induced and largest absolute ramp (Fig. 5a) and January 4th was also in the top 4 for both (Fig. 5c). Therefore, similar to Fig. 5, Fig. 9 shows daily profiles for the remaining days when the largest weather-induced ramps were observed. SAW estimates tracked the CSI power output typically within 6-7% rMAE at 30-min resolution.

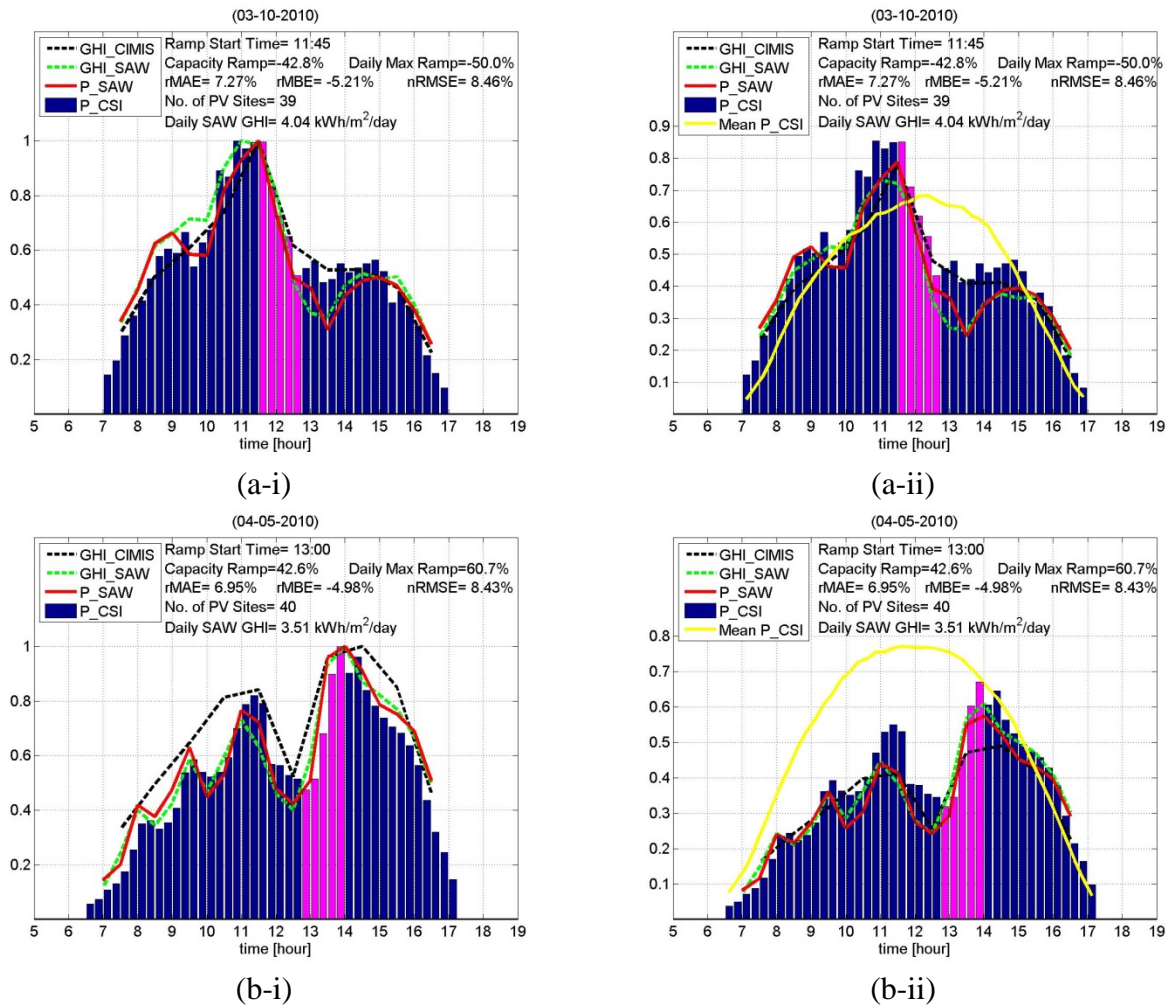


Fig. 9: Days with the 2nd and 3rd largest weather-induced ramps: Same as Fig. 5 but for weather-induced ramp rates (aggregate power output minus 30 day average diurnal power output). (a) Mar. 10, 2010 and (b) Apr. 5, 2010. The (ii) graphs also show the 30 day average diurnal power output (yellow lines) and are not normalized to 1.

3.3. Marine layer breakup

While it did not cause *the* largest ramp, marine layer breakup caused most of the large ramps occurring during May through November and two of the four largest ramps (Sep 18 and Aug 12). The morning marine layer breakup is responsible for the majority of large ramps being up-ramps in Fig. 4 during those months. The 15 minute consecutive GOES images for the time period with the second largest absolute ramp (Fig. 5b, as an example of marine layer cloud breakup) are illustrated in Fig. 10. A large morning up-ramp (44% of installed PV capacity per hour) occurred due to marine layer retreat that occurs over 2 hours (8am-10am).

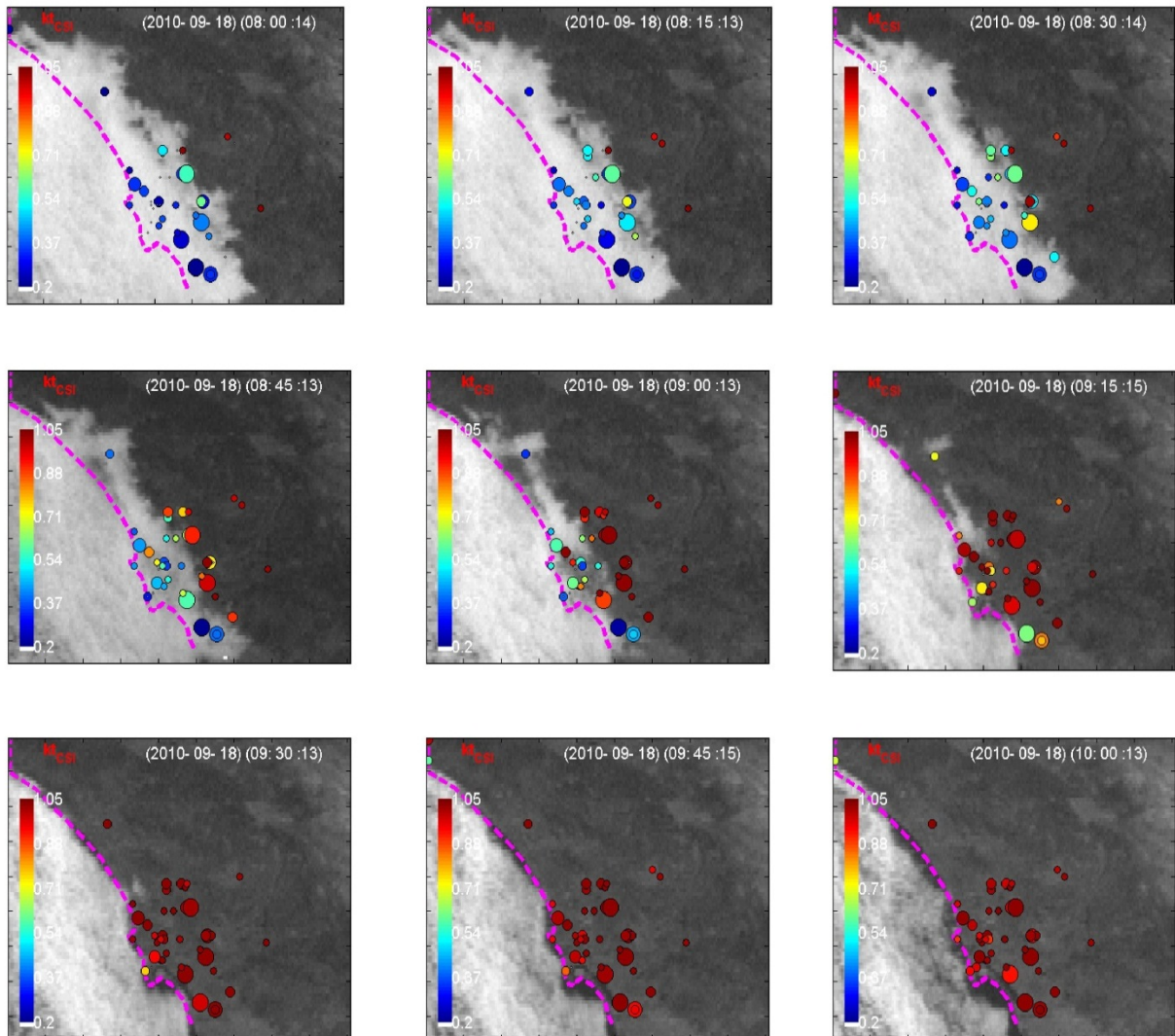


Fig. 10: GOES images for a day with marine layer breakup (second largest absolute ramp): Same as Fig. 6 but for Sep. 18, 2010 (Fig. 5b). The largest aggregated 1 hour absolute ramp for this period was 44% of PV capacity and occurred from 830 to 930 PST.

4. Conclusions

Aggregate ramp rates of 45 PV systems installed in SDG&E territory were presented and compared to satellite-derived Solar Anywhere irradiation and measured GHI at 5 weather stations (CIMIS).

The PV performance model applied to the satellite solar resource data was able to follow the power output measured over 45 systems typically within 1-12% during the four largest ramps. The largest hourly absolute and weather-induced ramps were 60% and 55% of PTC capacity respectively. In a very high PV penetration scenario, if such ramps hit the operator unprepared, they may indeed cause reliability challenges and additional costs for the system operator.

However, many of the largest ramp rates are caused by summer marine layer breakup when cloud evaporation coincides with an increase in solar altitude nearly every morning (e.g. the day with the second and fourth largest absolute ramp). During the winter months, the ramp rates are mainly caused by the winter frontal storm systems; when fast-moving storm systems move into the area (creating a large down ramp) or out of the area (creating a large up-ramp).

This analysis was focused on distributed generation systems that are relatively well distributed across the state. Groups of larger but less geographically diverse systems may experience larger weather induced ramps.

5. References

1. California Solar Initiative, "California Public Utilities Commission California Solar Initiative Program Handbook," Accessed Sep. 2011 at: http://www.gosolarcalifornia.org/documents/CSI_HANDBOOK.PDF
2. Itron, Inc. & KEMA, Inc., "CPUC California Solar Initiative 2009 Impact Evaluation," Jun. 2010. Available: http://www.cpuc.ca.gov/NR/rdonlyres/70B3F447-ADF5-48D3-8DF0-5DCE0E9DD09E/0/2009_CSI_Impact_Report.pdf
3. J. Luoma and J. Kleissl, Summary of Quality Control for 2010 CSI Data, Internal Report, 2012.
4. CIMIS Sensor Specifications. Accessed on Mar 15 2011 at: <http://www.cimis.water.ca.gov/cimis/infoStnSensorSpec.jsp>.
5. D.W. Meek and J.L. Hatfield, "Data quality checking for single station meteorological databases," *Agricultural and Forest Meteorology* 69 (1-2), 85-109, 1994.
6. S.O. Eching and D. Moellenberndt, "Technical Elements of CIMIS, the California Irrigation Management Information System: State of California, Resources Agency, Dept. of Water Resources, Division of Planning and Local Assistance," 66, 1998.
7. M. Jamaly and J. Kleissl, Validation of SolarAnywhere Enhanced Resolution Irradiation in California, Internal Report, 2012.
8. Web-based Clean Power Research service database, SolarAnywhere. Available: <https://www.solaranywhere.com/Public/About.aspx>
9. Perez, R., Ineichen, P., Moore, K., Kmiecik, M., Chain, C., George, R., and Vignola, F., "A new operational model for satellite-derived irradiances: Description and validation," *Solar Energy*, 73(5):307-317, 2002.
10. M. Jamaly, J.L. Bosch, and J. Kleissl, Power Output Analysis of Distributed PV Systems in California Using SolarAnywhere Enhanced Resolution Irradiation, Internal Report, 2012.

11. P. Ineichen, "Comparison of eight clear sky broadband models against 16 independent data banks," Solar Energy, 80:468–478, 2006.
12. Solar Radiation Database (SoDa). Available: <http://www.soda-is.com>.

Appendix A: Aggregate Power Output and Irradiances for the four Days with the Largest Hourly Absolute Ramps

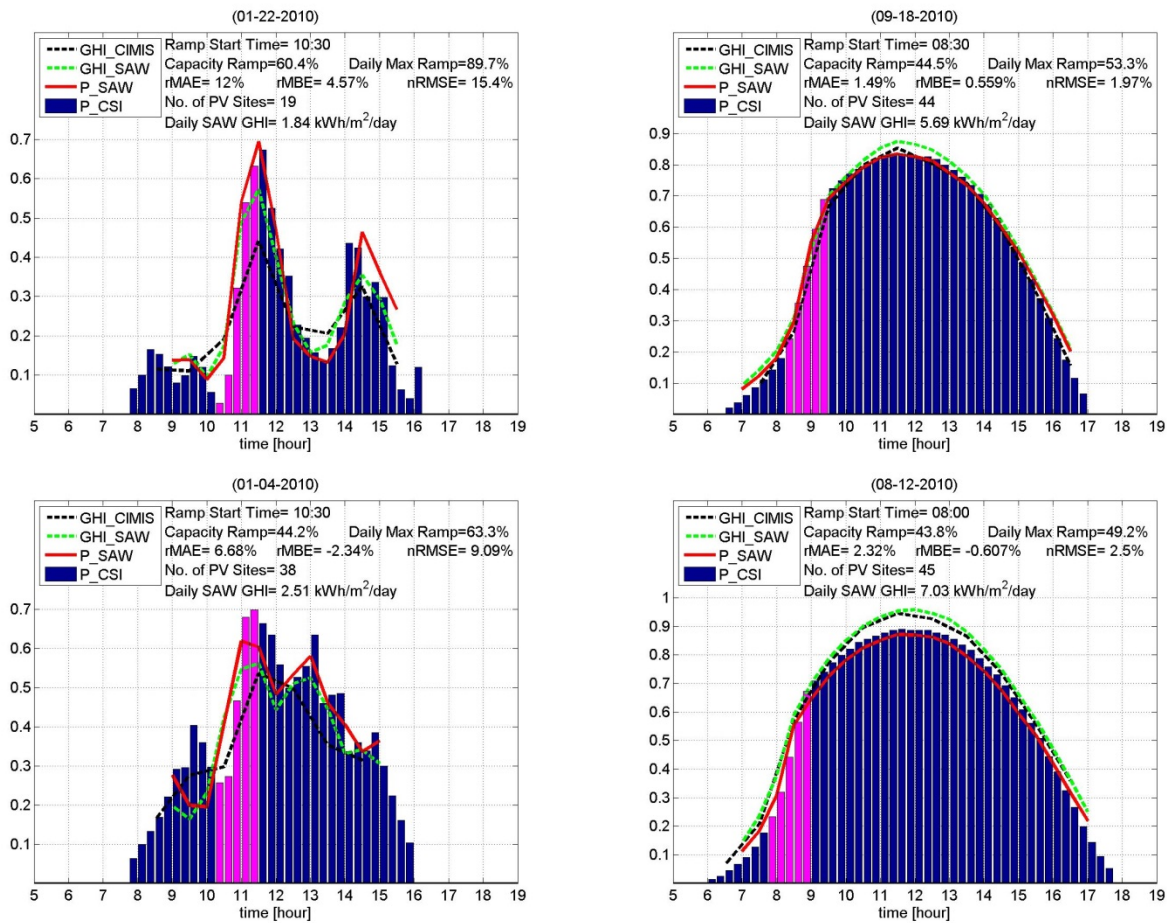


Fig. A1: Same as Fig. 5, but for aggregate CSI measured and SAW modeled power outputs (normalized by kW_{AC}) along with the aggregate SAW and CIMIS GHI (divided by 1000 W m^{-2}). Note that irradiances (GHI) are not expected to match power output since the power output is from a tilted surface.